Sakarya Üniversitesi Fen Bilimleri Dergisi
Sakarya University Journal of Science

e-ISSN : 2147-835X
Publisher : Sakarya University

Vol. 29, No. 5, 510-521, 2025
DOI: https://doi.org/10.16984/saufenbilder.1617813

Research Article

Investigation of Thermal and Mechanical Behaviors of Plaster Mixed with Granite Cutting Waste

Onur Yontar[1], Arife Kübra Yontar[2*], Emre Şirin[3]

[1] Department of Mechanical Engineering, Ondokuz Mayıs University, Samsun, Türkiye, onur.yontar@omu.edu.tr, ror.org/028k5qw24
[2] Department of Mechanical and Metal Technologies, Ondokuz Mayıs University, Samsun, Türkiye, kubra.demirbas@omu.edu.tr, ror.org/028k5qw24
[3] Samsun Anakent Turizm Ticaret A.Ş, Samsun, Türkiye, emre_s_irin@outlook.com
[*]Corresponding Author

ARTICLE INFO

Keywords:
Granite cutting waste
Plaster
Thermal conductivity
Compressive strength

Article History:
Received: 11.01.2025
Revised: 02.08.2025
Accepted: 08.09.2025
Online Available: 20.10.2025

ABSTRACT

This study investigated the usability of granite cutting waste in plaster. In the samples produced in the study, granite dust was observed with a scanning electron microscope, and it was homogeneously distributed in the microstructures. The presence of calcite, quartz, portlandite, hematite, and magnesium oxide phases in the samples was detected with an X-ray diffractometer. It was calculated that the highest compressive strength was obtained by adding 30% granite dust. In the samples whose thermal conductivities were examined by imaging with a thermal camera, it was determined that the lowest conductivity belonged to the sample containing 30% granite dust. This study revealed that plaster with high mechanical strength and low thermal conductivity could be produced by adding 30% granite dust.

1. Introduction

Plasters are frequently utilized in building construction because of their simple production method, widespread availability, cost-effectiveness, and better fire resistance. Gypsum-based plasters are commonly used as the principal interior finish for building wall and ceiling surfaces. Furthermore, with the proper method, it may be recycled numerous times [1–3].

Plaster (β-$CaSO_4$ 0.5H_2O) is prepared at a particular calcination temperature for large-scale applications using phosphor as the basic material. Plaster offers numerous benefits, including being lightweight, having excellent temperature resistance, and being low cost. The packing density of a board made from plaster is approximately 1 g/cm^3. Gypsum-based materials can resist temperatures up to 200 °C without significant damage and retain 50% of their genuine toughness at 400 °C. However, due to its disadvantages such as inherent brittleness, short setting time, poor water resistance, low resistance to cracking and inability to withstand humid conditions, gypsum plaster becomes an undesirable product for exterior plaster applications [4, 5]. Studies have been conducted with many natural and synthetic filling materials in recent years to increase plasters' thermal and mechanical resistance [6–8]. The most prominent of these filling materials are the cutting wastes of natural stones.

An igneous rock called granite is formed when some lava remains below the earth's surface and gradually cools to form crystalline rock. The primary chemical components of granite are magnesium oxide (MgO), calcium oxide (CaO), silicon dioxide (SiO_2), ferric oxide (Fe_2O_3), and aluminum oxide (Al_2O_3). SiO_2 makes up around 65–70% of the total, which is plentiful based on the chemical compositions above [9, 10]. Granite

Cite as: O. Yontar, A. K. Yontar, E. Şirin, "Investigation of thermal and mechanical behaviors of plaster mixed with granite cutting waste," Sakarya University Journal of Science, vol. 29, no. 5, pp. 510-521, 2025. https://doi.org/10.16984/saufenbilder.1617813

cutting waste, a byproduct of the mining industry, can replace aggregate materials in concrete mass production to some extent (or entirely). Granite waste is made up of both solid and sludge. Granite colloidal waste accounts for around 58% of total plant output and is typically disposed of in dumping zones.

Unfortunately, the rising buildup of non-biodegradable wastes over landfill sites poses major environmental concerns and contamination in the adjacent regions [11, 12]. Although granite mud is thought to be inert and non-toxic, its inconsiderate manufacturing and improper disposal cause difficulty and costs for businesses in addition to a host of adverse environmental effects, including altered soil drainage conditions, air and visual pollution, alteration and destruction of the natural landscape, and harm to human health because the mud dries and turns into a powder that may result in silicosis if inhaled [13]. As a result, granite waste has been classified as an airborne and hazardous substance that generates air pollution and lung and sinus ailments, decreases soil porosity, contaminates subterranean water, and interrupts the normal flow of aquifers [14, 15].

Many forms of non-biodegradable waste are discharged into the environment due to stone mining and processing. Over several years, gathering these wastes from the stone business has caused environmental damage in various ways. Waste recycling has been strongly encouraged across the industrial chain in recent years. It is a particularly efficient method to mitigate the consequences of large-scale raw material utilization and waste generation.

Construction is one of the industries with the most significant environmental impact, accounting for 75% of all natural resources removed from the earth. As a result, it has become critical to discover safe disposal techniques or recycling in the business for some high-value goods [16, 17]. Over the last decade, the granite mining sector has increased by roughly 6% of global output each year, and granite waste from processing is estimated to represent about half of the finished granite quantity. Because using granite stone as a construction and architectural material creates significant waste during mining and processing, discovering new applications might decrease potential environmental contamination and raw material requirements [17].

The literature has limited knowledge and experimental data on the usage and effects of granite cutting remains in plaster. In light of the aforementioned information, the use of granite cutting waste in plaster and its impact on plaster's thermal and mechanical properties were investigated in this study. It has been a valuable step in reducing manufacturing waste and developing new-generation building materials.

2. Materials and Methods

2.1.Preparation of samples

Commercial plaster was used to prepare the samples. Samsun Anakent Turizm Ticaret A.Ş., a Samsun Metropolitan Municipality state-owned enterprise, supplied granite cutting wastes. The granite cutting waste used are shown in Figure 1 (a). The samples were prepared in 50 x 50 x 50 mm cubic plastic molds. The sample (P) without granite cutting waste was prepared as a control sample. Granite cutting waste were added to the plaster at 15, 30 and 45 wt%. After mixing, the granite cutting waste and water were poured into the mold, as shown in Figure 1 (b). The samples dried in the mold for a day and then dried at room temperature for 6 days. The ratios used to prepare the samples are given in Table 1.

2.2.Characterizations and tests

A scanning electron microscope (SEM) model (JEOL 7001F) equipped with an EDS analysis adapter and an 80 mm^2 X-MAX detector was used to evaluate the chemical composition and microstructure of the samples. After the compression test, an SEM examination was performed to determine the structure and distribution of the broken pieces from all samples. The resolution was measured under 5 and 10 kV acceleration voltage. The pieces taken for imaging in the SEM were coated with gold and palladium. EDS spectra and map analysis were used to determine the chemical contents of the granite particles and how they were distributed throughout the samples. XRD

analysis was performed using a Rigaku Smart Lab CuK radiation monochromatic filter device in the range of 10°–70° at room temperature, 2°/min speed, and 1.2 Å wavelength to determine the phases in and granite found in the samples. XRD data were collected using 2D HyPix-3000 area detectors. The Debye-Scherrer Equation (1) was used to calculate the crystallite size and microstrain of the samples. The Debye-Scherer equation;

$$D = K\lambda/\beta\cos\theta \quad (1)$$

Table 1. Sample names and quantities of ingredients used

Samples	Water (mL)	Plaster (g)	Granite (g)
P	200	300	-
PG15	200	255	45
PG30	200	210	90
PG45	200	165	135

where D is the crystallite size (nm), K is the so-called shape or geometry factor, which usually takes a value of about 0.9 (Scherer constant), λ the X-ray wavelength (k = 0.1541 nm), β the full width at half maximum (FWHM) of the diffraction peak, and "θ" the diffraction angle. Williamson-Hall (W–H) Equation (2) used for microstrain calculations. The microstrain values of crystallites have been calculated by using the W–H relation using the XRD peaks, and the equation is as follows;

$$B\cos\theta = \left(\frac{k\lambda}{D}\right) + 4\varepsilon\sin\theta \quad (2)$$
$$\text{Microstrain}(\varepsilon) = \beta/4\tan\theta$$

Compressive strengths of all samples were measured with a 6800 series INSTRON Universal testing machine. Three samples were prepared for each group. A total of 12 samples were subjected to compression testing, and the test speed was 3 mm/min. TESTO 881 thermal imager was used to examine the thermal conductivity properties of the samples. The upper surface of each sample was monitored by taking images with a thermal camera on a heated plate at 10-minute intervals for 1 hour. At the end of 1 hour, the temperature on the upper surface was recorded. The emissivity value was taken as 0.85 when making temperature measurements.

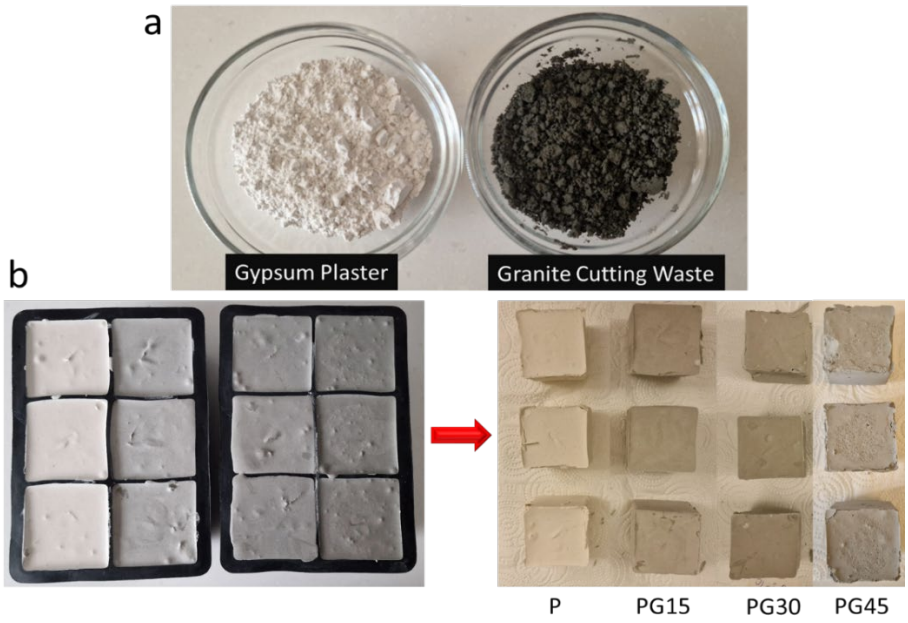

Figure 1. (a) Gypsum plaster and granite cutting wastes, (b) Samples in mold and dried samples

3. Results and Discussion

3.1.Scanning Electron Microscope (SEM)

After the compression test, SEM analysis was performed on the broken pieces to examine how the particles of plaster and granite were distributed within the structure. Since this distribution affects the samples' compression strength and thermal properties, it is crucial to examine the SEM images. The structure of the sample without granite in Figure 2 (a) shows that the waste particles are in rectangular and square-shaped crystal-like structures. As seen in Figure

2 (b) of the PG15 sample microstructure, granite particles with lighter colors and smaller sizes are scattered among the particles. Similarly, in the SEM images of Figure 2 (c) and (d), it was observed that the granite particles were dispersed among the particles but were more concentrated.

It was determined that the granite particles were homogeneously distributed throughout the structure of the PG45 sample, which had the highest amount of granite. It was also determined that the particles were dispersed quite a lot from each other due to the high granite ratio. In general, it has been determined that granite particles exhibit a homogeneous distribution in the structure, and their sizes are much smaller than those of particles, on average 1-2 µm.

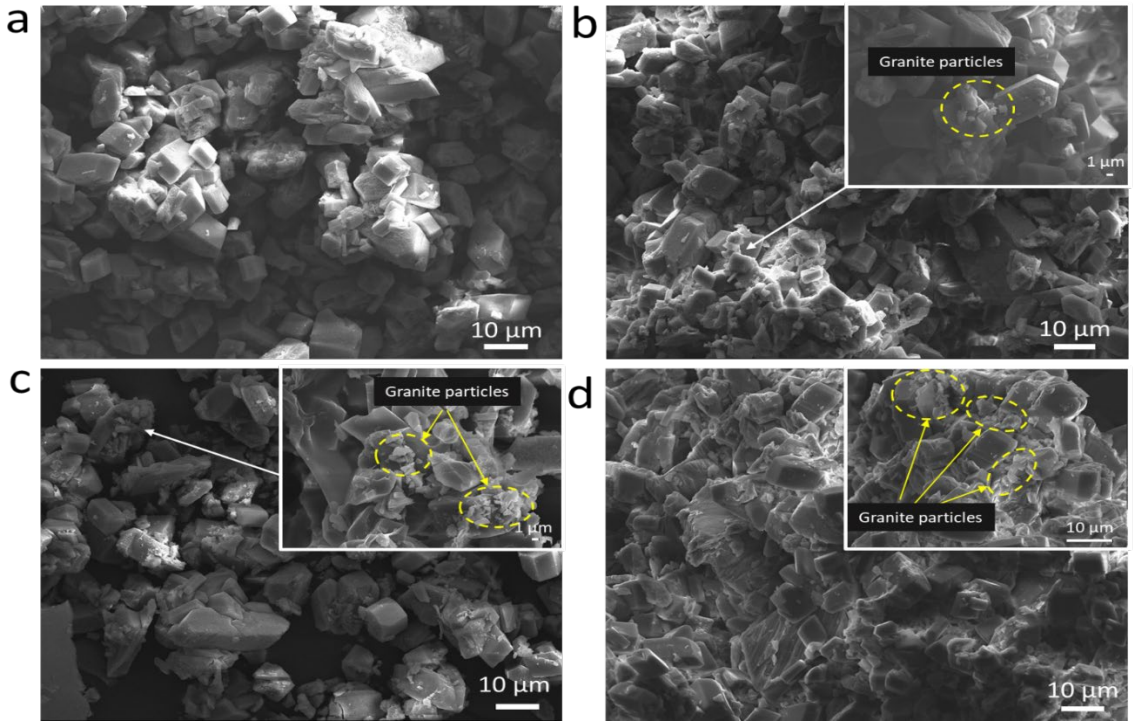

Figure 2. SEM images of (a) P, (b) PG15, (c) PG30 and (d) PG45 samples

3.2.Energy Dispersive Spectrometry (EDS)

The results of the EDS analysis performed to determine the elemental composition of blocks produced from granite are shown with the mapping method in Figure 3. The distributions of the elements found in the entire sample are given together with their percentages. Figure 3(a) shows the EDS mapping results of sample P that does not contain granite waste. Plaster is mainly made of calcium sulfate hemihydrate ($CaSO_4$ $_2H_2O$) [18, 19]. The elements C, Ca, O and S seen in the map spectrum reveal that the material used in this sample is plaster. Granite's primary chemical ingredients are calcium oxide (CaO), silicon dioxide (SiO_2), aluminum oxide (Al_2O_3), ferric oxide (Fe_2O_3), and magnesium oxide (MgO). According to the formulas for substances above, SiO_2 is plentiful, accounting for 65 to 70% of the total [20, 21]. Figures 3 (b), (c), and (d) show the presence of Si, Al, Mg, Fe, K, and Na elements coming from granite, in addition to C, Ca, O, and S elements belonging to, in samples containing granite cutting waste.

Table 2. Chemical composition of granite cutting waste

Element	Wt%
P	56.37
O	0.58
Na	3.52
Mg	3.84
Al	8.52
Si	8.35
S	2.05
K	10.34
Ca	0.64
Ti	0.46
Cr	5.33
Fe	56.37

According to the EDS spectrum analysis results, the chemical composition of the granite cutting wastes used in the study is shown in Table 2. The results of EDS spectrum analyses performed to detect granite particles in samples containing granite cutting waste are given in Figure 4. The large dark particles seen in SEM images are mainly composed of C, Ca, O and S, while other small light-colored particles are particles containing high amounts of Fe, Si, Mg, Na, Al, Ti and K, and these elements belong to granite cutting waste. It is estimated that elements such as Ti and Cr are present due to contamination from cutting tools during cutting. Pd comes from the coating material used for SEM.

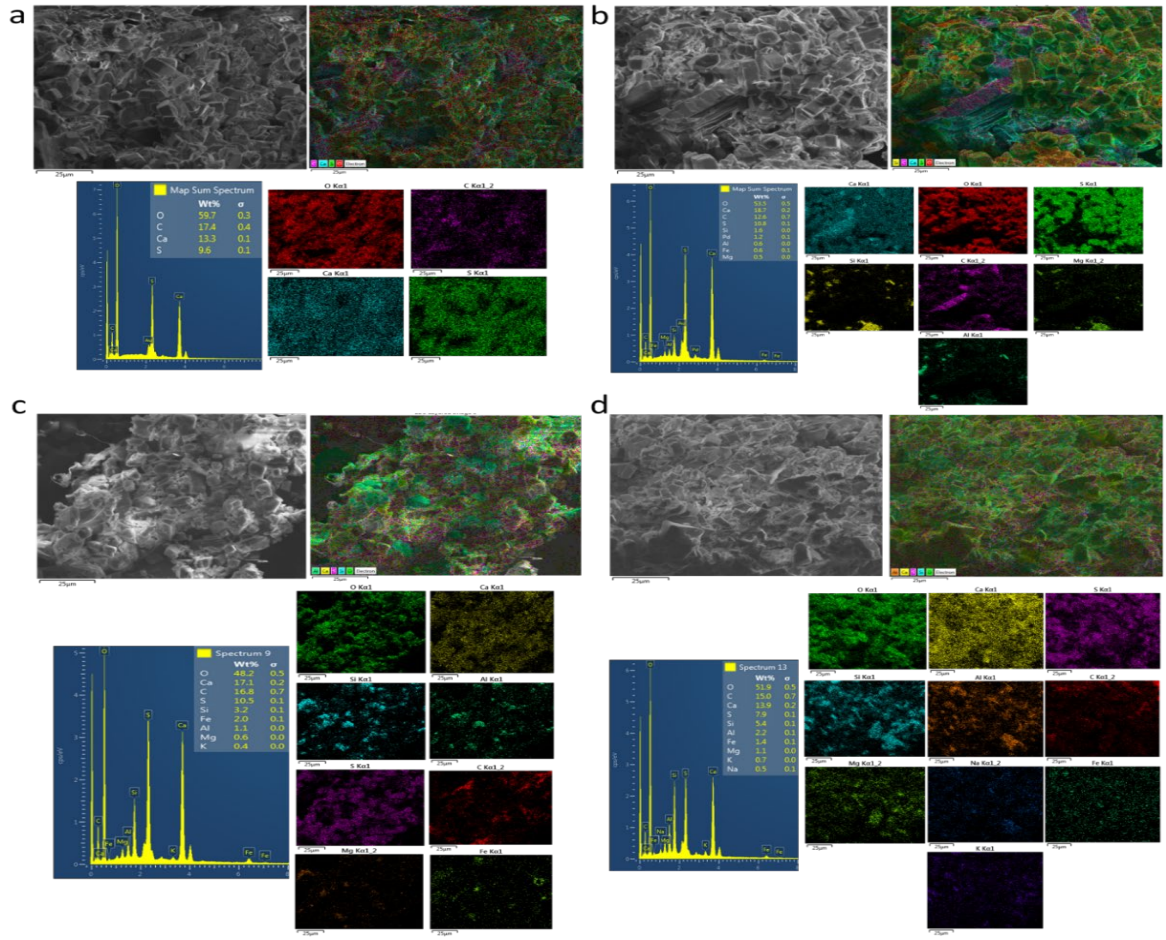

Figure 3. EDS mapping results (a) P, (b) PG15, (c) PG30 and (d) PG45 samples

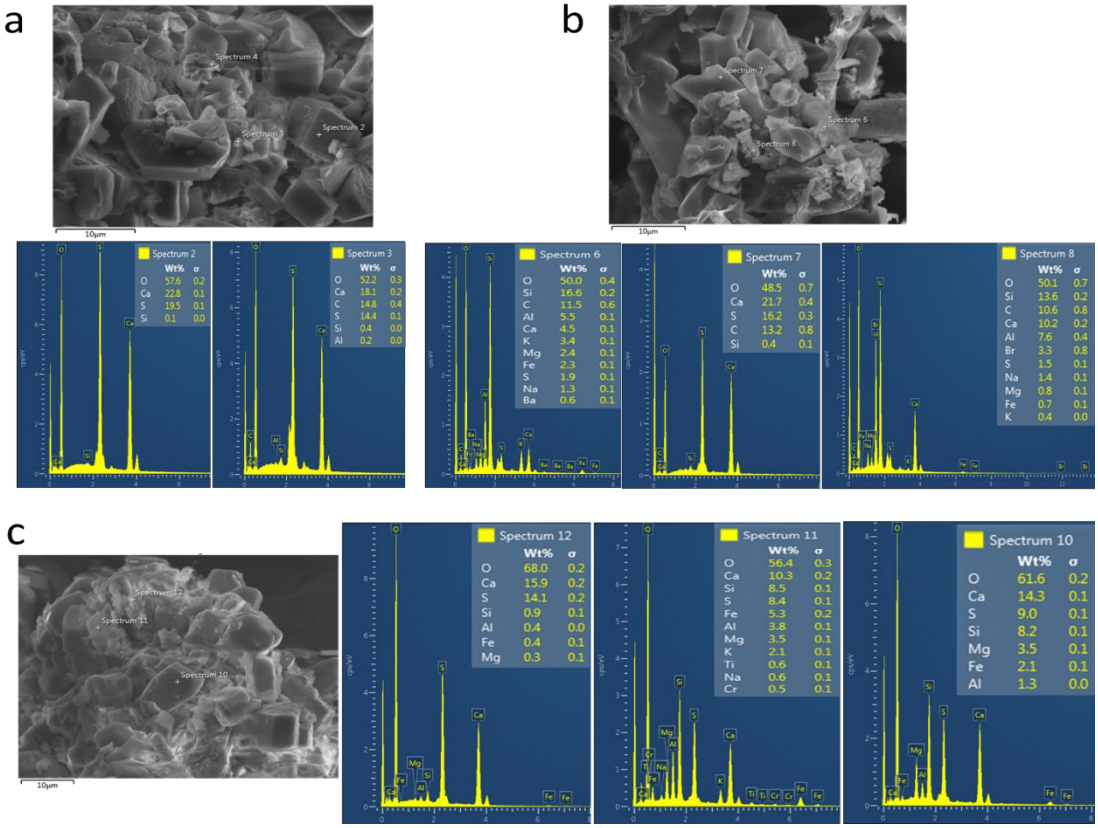

Figure 4. EDS spectrum results (a) PG15, (b) PG30, and (c) PG45 samples

3.3.X-Ray Diffraction analysis (XRD)

Figure 5 shows the XRD spectra of the samples. Since granite and plaster have similar chemical compositions, the peaks overlapped; therefore, no significant difference occurred. XRD peaks at 11.8˚, 23.6˚, 33.5˚, 36.1˚, 39.6˚, 43.5˚, 48˚, and 56.9˚ belong to calcite; peaks at 11.8˚, 31.1˚, 32.2˚, 43.5˚, 50.5˚, and 51.7˚ belong to dihydrate, peaks at 20.9˚, 23.6˚, 29.2˚, 39.6˚, 50.5˚, 51.7˚, and 55.3˚ belong to quartz, peaks at 23.5˚ and 48.6˚ belong to iron silicate, peak at 29.2˚ belongs to albite, peak at 33.5˚ belongs to portlandite, peaks at 33.5˚, 39.6˚, and 56.9˚ belong to silicon dioxide, peak at 40.9˚ belongs to hematite, and peak at 48.6˚ belongs to magnesium oxide phases [22–25].

All samples contain the phases and components of granite. As the amount of granite increases, the intensity of the quartz peaks decreases.
FWHM and the shape of the diffraction peak (size of the peak) reflect crystallinity. Perfect and blocky diffraction peaks occur in the presence of crystals as narrow vertical lines [26]. Figure 5 shows that XRD peaks have similar peak widths and power in all samples. In other words, the crystal structure ratio is high in all samples. It is seen that the crystallite sizes given in Table 3 are PG30<PG15<P<PG45, respectively.

The decrease in crystallite size causes an increase in microstrain in the structure. Because smaller sizes cause higher surface area and higher bond ratio and energy. Microstrain refers to the stresses that occur in crystals due to the stress within the material caused by non-homogeneous plastic deformation [27]. When the microstrain values of the samples were compared for all samples, it was determined that PG45<P<PG15<PG30 Crystallite sizes and microstrain results showed that while microstrain decreased in the PG45 sample compared to the P sample, microstrain increased in the PG15 and PG30 samples. During the compression test, the microstrain rises with increasing pressure in stronger samples. This suggests that granite cutting waste was better embedded in the plaster lattice in PG15 and PG30 samples, and therefore, their compressive strengths may have been higher [28]. Microstrain values were consistent with the compression test results.

Table 3. Sample names and quantities of ingredients used

Samples	Crystallite Sizes D (nm)	Microstrain (ε)
P	51.4	3.02 x 10^{-3}
PG15	51.2	3.04 x 10^{-3}
PG30	48.2	3.21 x 10^{-3}
PG45	51.9	2.9 x 10^{-3}

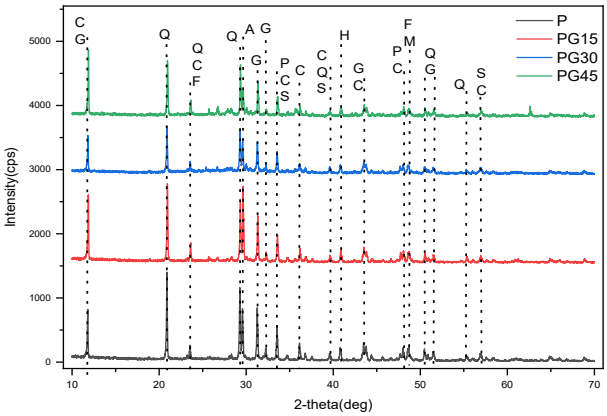

Figure 5. XRD results of all samples. (C: Calcite, Q: Quartz, G: dihydrate, F: Iron silicate, A: Albite, P: Portlandite, S: Silicon dioxide, H: Hematite, and M: Magnesium oxide)

3.4.Compressive strength

The results of all samples subjected to compression tests are given in the graphs in Figure 6, along with images of the samples after the test. The average compressive strength of the P sample was calculated as 0.53 MPa, the PG15 sample was 0.7 MPa, the PG30 sample was 0.74 MPa, and the PG45 sample was 0.39. It was determined that the amount of granite dust increased the compressive strength of the block by up to 30% while decreasing it by 45%.

This result showed that by adding 30% granite cutting waste into the plaster, a 39% increase in compressive strength could be achieved compared to the plaster sample without additives. The increase in strength of the PG30 sample is thought to be due to the finer inert particles of granite acting as nucleation points, causing the precipitation of hydrated products and activating the hydration [17]. The more prominent packing of the granite and plaster particles made the mixture more homogeneous and compact, thus exhibiting more excellent resistance. The strength of the PG45 sample decreased as the percentage of granite cutting waste was raised to 45%. Because plaster has strong binding qualities, lowering its concentration in the sample also decreased the quantity of bond that was produced between the plaster and the granite cutting waste. It has been reported in similar studies that the decrease in the amount of binder or its non-homogeneous distribution reduces the compressive strength [29, 30].

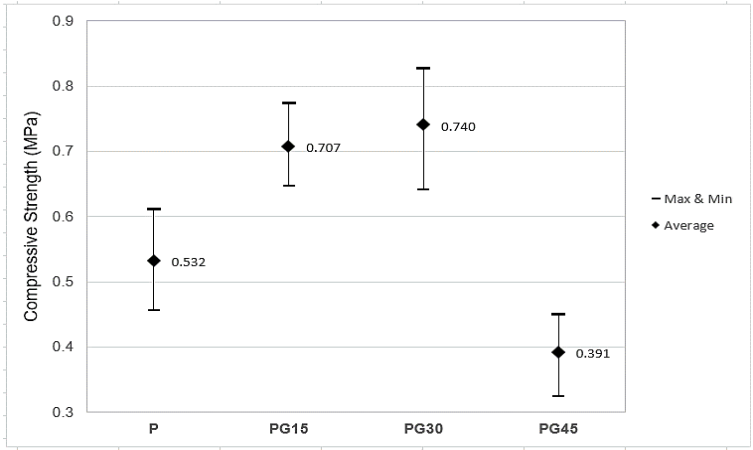

Figure 6. Compressive test result graphs of all samples

3.5.Thermal conductivity

To compare the thermal conductivities of the samples, each sample was placed on a heater heated to 100 ˚C and then kept for 1 hour. Measurements were taken with a thermal camera every 10 minutes, and the temperature changes between the bottom and top surfaces of the samples were recorded for one hour, as shown in the thermal camera images in Figure 7. For each sample, temperature changes were measured from 3 different points from the bottom to the top surface. The measurement points were determined as point A, 1 cm above the bottom;

point B, 3 cm above the bottom; and point C, 5 cm above the bottom on the top surface of the sample.

Figure 7 shows that the temperature difference between the bottom and top surfaces of all samples at the 10th and 60th minutes was highest at 37.9 ˚C for the P sample and lowest at 25 ˚C for the PG30 sample. The temperature values measured for each point in the samples are given comparatively in the graphs in Figure 8. It was noticed that the temperatures of point A in PG15 and PG45 samples decreased after 40 minutes. It is predicted that this may be due to the temperature balance between points A and B being achieved after 40 minutes.

The lowest temperature increases at point B after 60 minutes were observed in the PG30 and PG45 samples. In other words, the temperature differences occurring in the inner parts of the square prism samples are lower than the pure P sample, indicating that the thermal conductivities of these samples are lower. In the temperature changes of the uppermost surface, point C, it was determined that the lowest temperature belonged to the PG30 sample. In the PG15 and PG45 samples, the temperature values measured at point C were higher than the P sample. The temperature differences measured at point A of the samples at the end of the 10th and 60th minutes were calculated as 9.5 ˚C for the P sample, 9.2 ˚C for PG15, 8.2 ˚C for PG30, and 12.4 ˚C for PG45. The total temperature differences occurring at points A were calculated as 19.5 ˚C for P, 11.8 ˚C for PG15, 8.1 ˚C for PG30, and 12.4 ˚C for PG45.

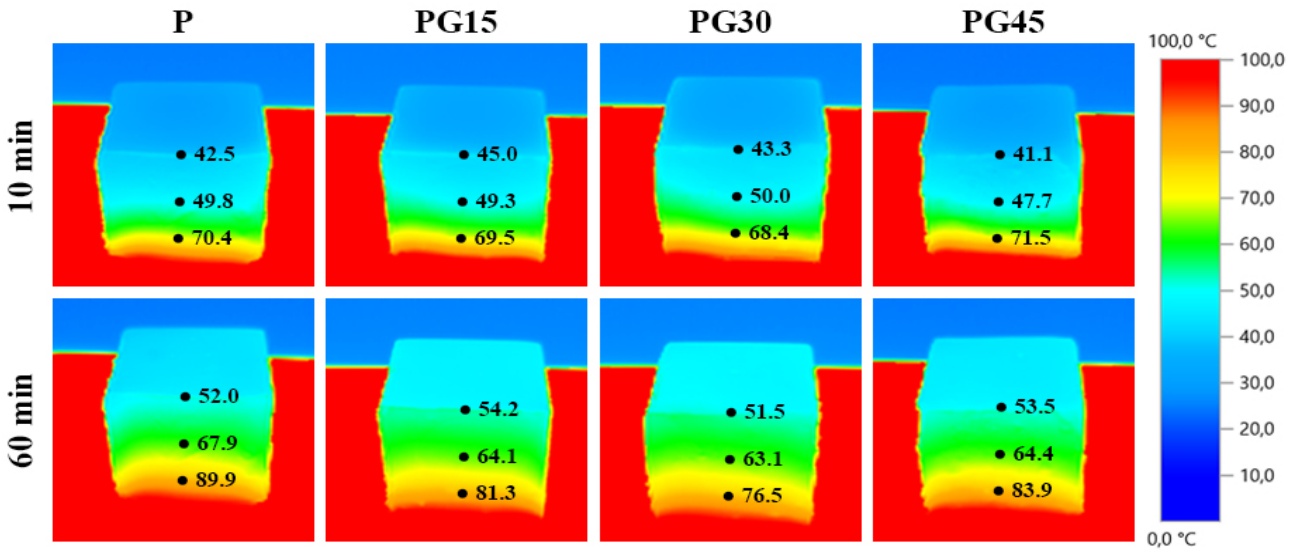

Figure 7. Thermal camera images of temperature changes of samples after 10 and 60 minutes

As a result, when all these temperature differences were compared, the thermal conductivity order between the samples was as follows: P>PG45>PG15>PG30. It was observed that a decrease in thermal conductivity occurred with the addition of granite cutting waste to the plaster. It was determined that the lowest thermal conductivity belonged to the PG30 sample. This decrease in thermal conductivity can be explained by the crystallite sizes and microstrain given in Table 2. The lowest crystallite size and the highest microstrain belong to the PG30 sample.

It is hypothesized that smaller-sized crystallites were created by mixing granite cutting waste with plaster and that increased porosity occurred in the structure with these combinations and agglomerations [31, 32]. Moreover, these agglomerations also led to higher microstrains in the structure. Therefore, it is thought that the thermal conductivity may have decreased with the increase in porosity and voids.

4. Conclusion

This study investigated the use of granite cutting waste in plaster for recycling. The characterizations, mechanical strengths, and thermal properties of the samples added to plaster

at 15%, 30%, and 45% were examined. SEM analysis showed that granite dusts were homogeneously distributed in plaster. EDS mapping and spectrum analysis revealed the presence of granite dust and Si, Al, Mg, Fe, K, Na, C, Ca, O, and S elements from both granite and plaster.

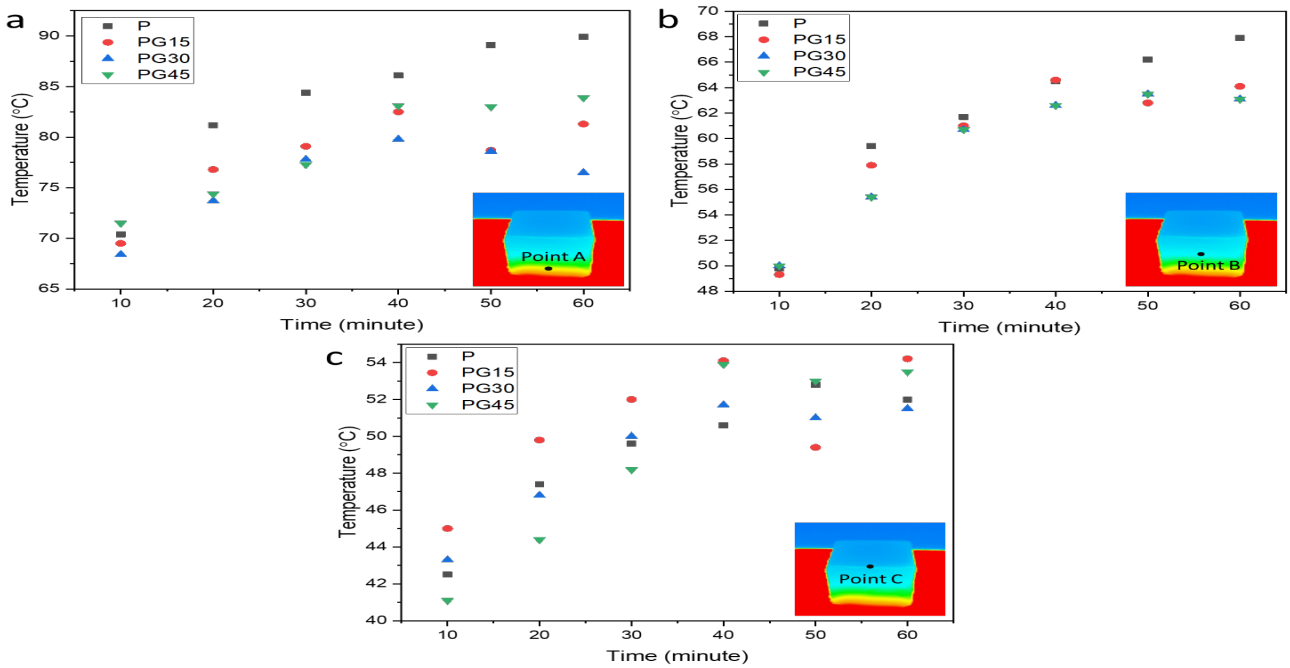

Figure 8. Graphs of temperature changes on surfaces (a) Point A, (b) Point B, and (c) Point C

In addition, XRD proved that the dust used in the study belonged to granite, with calcite, hematite, dihydrate, iron silicate, silicon dioxide, albite, portlandite, and magnesium oxide peaks. It was determined that the compressive strengths of the samples produced in the form of 50 x 50 mm cube blocks increased with granite dust. In particular, it was calculated that the PG30 sample containing 30% granite dust had the highest compressive strength with 0.74 MPa. It was determined that adding more granite dust than this rate reduced the compressive strength of the plaster.

When thermal properties were examined, it was found that thermal conductivities decreased with the addition of granite cutting waste. The lowest thermal conductivity belonged to the PG30 sample. Thus, it was concluded that the compressive strength of the plaster was increased, and its thermal conductivity was reduced with the addition of 30% granite cutting waste.

This study paves the way for evaluating granite cutting waste using it in plaster. With the findings obtained in the study, it was possible to produce materials with superior properties while reducing waste formation.

Article Information Form

Acknowledgments
The granite cutting waste used in this study were supplied by Samsun Anakent Turizm Ticaret A.Ş., which belongs to Samsun Metropolitan Municipality.

Authors' Contribution
Onur Yontar: Methodology, Research, Data editing, Manuscript writing and editing, Arife Kübra Yontar: Methodology, Research, Data editing, Manuscript writing and editing, Experimental Study, Emre Şirin: Methodology and Granite powder supply.

The Declaration of Conflict of Interest/ Common Interest
No conflict of interest or common interest has been declared by authors.

Artificial Intelligence Statement
No artificial intelligence tools were used while writing this article.

References

[1] H. E. Benchouia, H. Boussehel, B. Guerira, L. Sedira, C. Tedeschi, H. E. Becha, M. Cucchi, "An experimental evaluation of a hybrid bio-composite based on date palm petiole fibers, expanded polystyrene waste, and gypsum plaster as a sustainable insulating building material," Construction and Building Materials, vol. 422, p. 135735, 2024.

[2] K. Elert, P. Bel-Anzué, M. Burgos-Ruiz, "Influence of calcination temperature on hydration behavior, strength, and weathering resistance of traditional gypsum plaster," Construction and Building Materials, vol. 367, pp. 130361, 2023.

[3] M. Hagiri, K. Honda, "Preparation and evaluation of gypsum plaster composited with copper smelter slag," Cleaner Engineering and Technology, vol. 2, pp. 100084, 2021.

[4] L. Wang, M. Cao, X. Li, W. Du, X. Wang, "A novel approach for improving the water resistance of gypsum plaster by internal mixing hypromellose and external coating waterproofing agent," Construction and Building Materials, vol. 401, pp. 132940, 2023.

[5] S. Bouzit, F. Merli, M. Sonebi, C. Buratti, M. Taha, "Gypsum-plasters mixed with polystyrene balls for building insulation: Experimental characterization and energy performance," Construction and Building Materials, vol. 283, pp. 122625, 2021.

[6] J. Zehfuß, L. Sander, "Gypsum plasterboards under natural fire—Experimental investigations of thermal properties," Civil Engineering Design, vol. 3, no. 3, pp. 62-72, 2021.

[7] N. C. Amulah, A. M. El-Jummah, A. A. Hammajam, U. Ibrahim, "Experimental Investigation on the Thermal Properties of Gypsum Plaster-Rice Husk Ash Composite," Open Journal of Composite Materials, vol. 12, no. 04, pp. 131-138, 2022.

[8] Y. Agrawal, S. Siddique, R. K. Sharma, T. Gupta, "Valorization of granite production dust in development of rich and lean cement mortar," Journal of Material Cycles and Waste Management, vol. 23, no. 2, pp. 686-698, 2021.

[9] K. Shwetha, C. Mahesh Kumar, V. N. Dalawai, S. Anadinni, G. Sowjanya, "Comparative study on strengthening of concrete using granite waste," Materials Today: Proceedings, vol. 62, pp. 5317-5322, 2022.

[10] A. A. Mhamal, P. P. Savoikar, "Use of marble and granite dust waste as partial replacement of fine aggregates in concrete," IOP Conference Series: Earth and Environmental Science, vol. 1130, no. 1, pp. 12013, 2023.

[11] S. Tangaramvong, P. Nuaklong, M. T. Khine, P. Jongvivatsakul, "The influences of granite industry waste on concrete properties with different strength grades," Case Studies in Construction Materials, vol. 15, pp. 00669, 2021.

[12] M. A. Pedreño-Rojas, C. Rodríguez-Liñán, I. Flores-Colen, J. de Brito, "Use of Polycarbonate Waste as Aggregate in Recycled Gypsum Plasters," Materials (Basel, Switzerland), vol. 13, no. 14, 2020.

[13] F. Oliveira, R. Sousa, P. Silva, P. Lopes, G. Moreira, R. Leite, R. Arruda, "Analysis of the benefits of the addition of granite residues in the production of ecological brick," International Journal of Advanced Engineering Research and Science, vol. 8, no. 3, pp. 149-158, 2021.

[14] K. Weimann, C. Adam, M. Buchert, J. Sutter, "Environmental Evaluation of Gypsum Plasterboard Recycling," Minerals, vol. 11, no. 2, pp. 101, 2021.

[15] B. Ngayakamo, A. Bello, A. P. Onwualu, "Valorization of granite waste powder as a secondary flux material for sustainable production of ceramic tiles," Cleaner Materials, vol. 4, pp. 100055, 2022.

[16] A. S. Nascimento, C. P. dos Santos, F. M. C. de Melo, V. G. A. Oliveira, R. M. P. Betânio Oliveira, Z. S. Macedo, H. A. de Oliveira, "Production of plaster mortar with incorporation of granite cutting wastes," Journal of Cleaner Production, vol. 265, pp. 121808, 2020.

[17] M. R. Gehlot, S. Shrivastava, "Utilization of stone waste in the development of sustainable mortar: A state of the art review," Materials Today: Proceedings, 2023.

[18] N. Kondratieva, M. Barre, F. Goutenoire, M. Sanytsky, "Study of modified gypsum binder," Construction and Building Materials, vol. 149, pp. 535-542, 2017.

[19] A. Erbs, A. Nagalli, K. Querne de Carvalho, V. Mymrin, F. H. Passig, W. Mazer, "Properties of recycled gypsum from gypsum plasterboards and commercial gypsum throughout recycling cycles," Journal of Cleaner Production, vol. 183, pp. 1314-1322, 2018.

[20] G. Amulya, A. A. B. Moghal, A. Almajed, "A State-of-the-Art Review on Suitability of Granite Dust as a Sustainable Additive for Geotechnical Applications," Crystals, vol. 11, no. 12, pp. 1526, 2021.

[21] A. A. Mahmoud, A. A. El-Sayed, A. M. Aboraya, I. N. Fathy, M. A. Abouelnour, I. M. Nabil, "Influence of sustainable waste granite, marble and nano-alumina additives on ordinary concretes: a physical, structural, and radiological study," Scientific reports, vol. 14, no. 1, pp. 22011, 2024.

[22] M. E. Tawfik, S. B. Eskander, N. M. Ahmed, "Potential applications of granite waste powder as an add-value polymer composite product," Polymers and Polymer Composites, vol. 30, 2022.

[23] R. Saxena, T. Gupta, R. K. Sharma, S. Siddique, "Mechanical, durability and microstructural assessment of geopolymer concrete incorporating fine granite waste powder," Journal of Material Cycles and Waste Management, vol. 24, no. 5, pp. 1842-1858, 2022.

[24] C. Y. Rahimzadeh, A. S. Mohammed, A. A. Barzinjy, "Microstructure characterizations, thermal analysis, and compression stress–strain behavior of lime-based plaster," Construction and Building Materials, vol. 350, pp. 128921, 2022.

[25] A. Jain, S. Chaudhary, R. Gupta, "Mechanical, microstructural characterization of fly ash blended self-compacting concrete containing granite waste," Construction and Building Materials, vol. 314, pp. 125480, 2022.

[26] Y. Zhang, Q. Sun, J. Geng, "Microstructural characterization of limestone exposed to heat with XRD, SEM and TG-DSC," Materials Characterization, vol. 134, pp. 285-295, 2017.

[27] Y.-J. Shen, Y.-L. Zhang, F. Gao, G.-S. Yang, X.-P. Lai, "Influence of Temperature on the Microstructure Deterioration of Sandstone," Energies, vol. 11, no. 7, pp. 1753, 2018.

[28] C. Pesce, G. L. Pesce, M. Molinari, A. Richardson, "Effects of organic additives on calcium hydroxide crystallisation during lime slaking," Cement and Concrete Research, vol. 139, pp. 106254, 2021.

[29] Z. Z. Woźniak, A. Chajec, Ł. Sadowski, "Effect of the Partial Replacement of Cement with Waste Granite Powder on the Properties of Fresh and Hardened Mortars

for Masonry Applications," Materials (Basel, Switzerland), vol. 15, no. 24, 2022.

[30] M. Sufian, S. Ullah, K. A. Ostrowski, A. Ahmad, A. Zia, K. Śliwa-Wieczorek, M. Siddiq, A. A. Awan, "An Experimental and Empirical Study on the Use of Waste Marble Powder in Construction Material," Materials (Basel, Switzerland), vol. 14, no. 14, 2021.

[31] M. I. Romero-Gómez, R. V. Silva, M. F. Costa-Pereira, I. Flores-Colen, "Thermal and mechanical performance of gypsum composites with waste cellulose acetate fibres," Construction and Building Materials, vol. 356, pp. 129308, 2022.

[32] K. Stejskalová, D. Bujdoš, L. Procházka, B. Smetana, S. Zlá, J. Teslík, "Mechanical, Thermal, and Fire Properties of Composite Materials Based on Gypsum and PCM," Materials (Basel, Switzerland), vol. 15, no. 3, 2022.